Silver(I) complexes with 4,7-phenanthroline efficient in rescuing the zebrafish embryos of lethal *Candida albicans* infection

Aleksandar Pavic[a,#,*], Nada D. Savić[b,#,*], Biljana Đ. Glišić[b], Aurélien Crochet[c], Sandra Vojnovic[a], Atanas Kurutos[d], Dalibor M. Stanković[e], Katharina M. Fromm[c], Jasmina Nikodinovic-Runic[a], Miloš I. Djuran[f,*]

[a]*Institute of Molecular Genetics and Genetic Engineering, University of Belgrade, Vojvode Stepe 444a, 11000 Belgrade*

[b]*University of Kragujevac, Faculty of Science, Department of Chemistry, R. Domanovića 12, 34000 Kragujevac, Serbia*

[c]*Department of Chemistry, University of Fribourg, Chemin du Musée 9, CH-1700 Fribourg, Switzerland*

[d]*Institute of Organic Chemistry with Centre of Phytochemistry, Bulgarian Academy of Sciences, Acad. G. Bonchev str., bl. 9, 1113 Sofia, Bulgaria*

[e]*The Vinča Institute of Nuclear Sciences, Mike Petrovića Alasa 12-14, 11000 Belgrade, Serbia*

[f]*Serbian Academy of Sciences and Arts, Knez Mihailova 35, 11000 Belgrade, Serbia*

[#]A.P. and N.D.S. contributed equally.

[*]Corresponding authors: Tel.: +381 11 397 6034; fax: +381 11 397 5808 (A. Pavic); Tel.: +381 34 336 223; fax: +381 34 335 040 (N. D. Savić); Tel.: +381 34 300 251; fax: +381 34 335 040 (M. I. Djuran).

E-mail addresses: sasapavic@imgge.bg.ac.rs (A. Pavic); nada.savic@kg.ac.rs (N. D. Savić); djuran@kg.ac.rs (M. I. Djuran).

Abstract

Five novel silver(I) complexes with 4,7-phenanthroline (4,7-phen), $[Ag(NO_3\text{-}O)(4,7\text{-phen-}\mu\text{-}N4,N7)]_n$ (**1**), $[Ag(ClO_4\text{-}O)(4,7\text{-phen-}\mu\text{-}N4,N7)]_n$ (**2**), $[Ag(CF_3COO\text{-}O)(4,7\text{-phen-}\mu\text{-}N4,N7)]_n$ (**3**), $[Ag_2(H_2O)_{0.58}(4,7\text{-phen})_3](SbF_6)_2$ (**4**) and $\{[Ag_2(H_2O)(4,7\text{-phen-}\mu\text{-}N4,N7)_2](BF_4)_2\}_n$ (**5**) were synthesized, structurally elucidated and biologically evaluated. These complexes showed selectivity towards *Candida* spp. in comparison to the tested bacteria and effectively inhibited the growth of four different *Candida* species, particularly of *C. albicans* strains, with minimal inhibitory concentrations (MICs) in the range of 2.0 – 10.0 μM. In order to evaluate the therapeutic potential of **1 – 5**, *in vivo* toxicity studies were conducted in the zebrafish model. Based on the favorable therapeutic profiles, complexes **1, 3** and **5** were selected for the evaluation of their antifungal efficacy *in vivo* using the zebrafish model of lethal disseminated candidiasis. Complexes **1** and **3** efficiently controlled and prevented fungal filamentation even at sub-MIC doses, while drastically increased the survival of the infected embryos. Moreover, at the MIC doses, both complexes totally prevented *C. albicans* filamentation and rescued almost all infected fish of the fatal infection outcome. On the other side, complex **5**, which demonstrated the highest antifungal activity *in vitro*, affected the neutrophils occurrence of the infected host, failed to inhibit the *C. albicans* cells filamentation and showed a poor potential to cure candidal infection, highlighting the importance of the *in vivo* activity evaluation early in the therapeutic design and development process. The mechanism of action of the investigated silver(I) complexes was related to the induction of reactive oxygen species (ROS) response in *C. albicans*, with DNA being one of the possible target biomolecules.

Keywords: Silver(I) complexes; Phenanthroline; DNA interaction; *Candida albicans*; *Danio rerio*; Infection model

TABLE OF CONTENTS

^{1}H NMR (400 MHz, DMF-d_7)

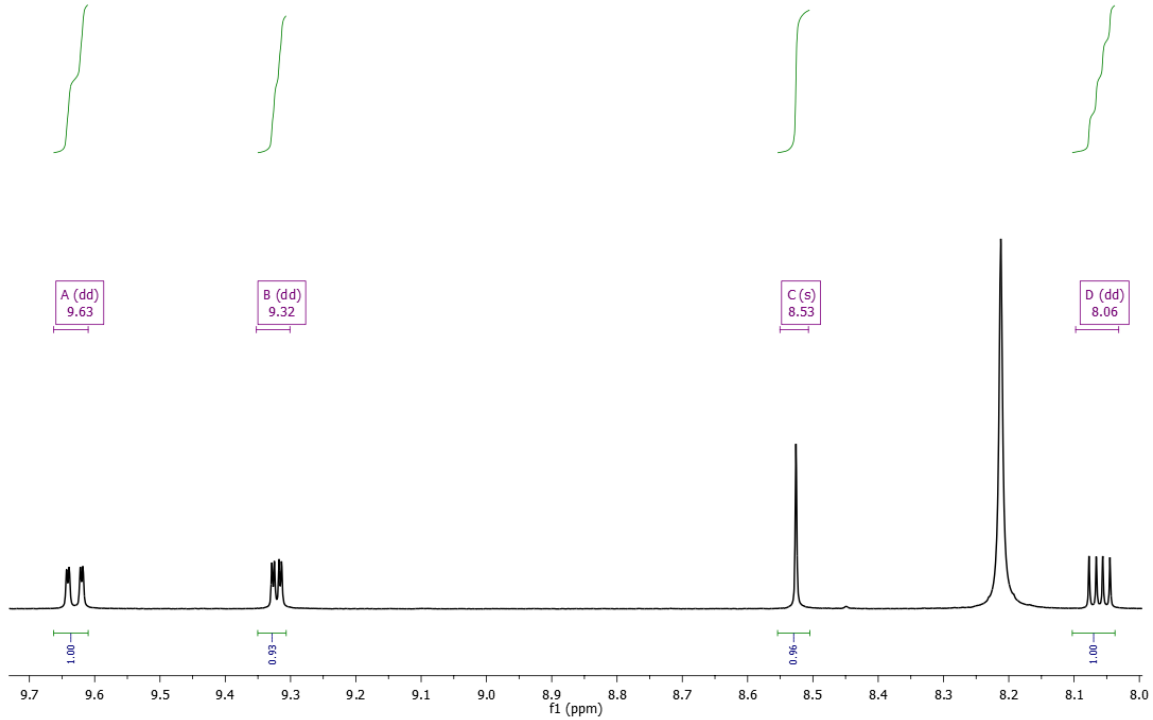

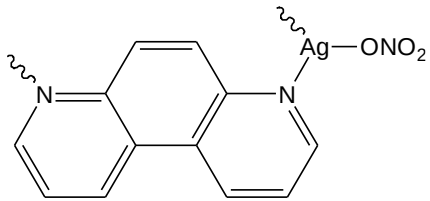

$[Ag(NO_3\text{-}O)(4,7\text{-phen-}\mu\text{-}N4,N7)]_n$

(1)

^{13}C NMR (101 MHz, DMF-d_7)

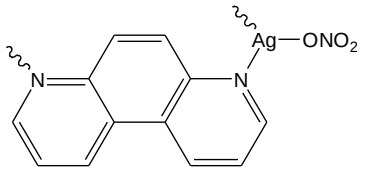

$[Ag(NO_3\text{-}O)(4,7\text{-phen-}\mu\text{-}N4,N7)]_n$

(1)

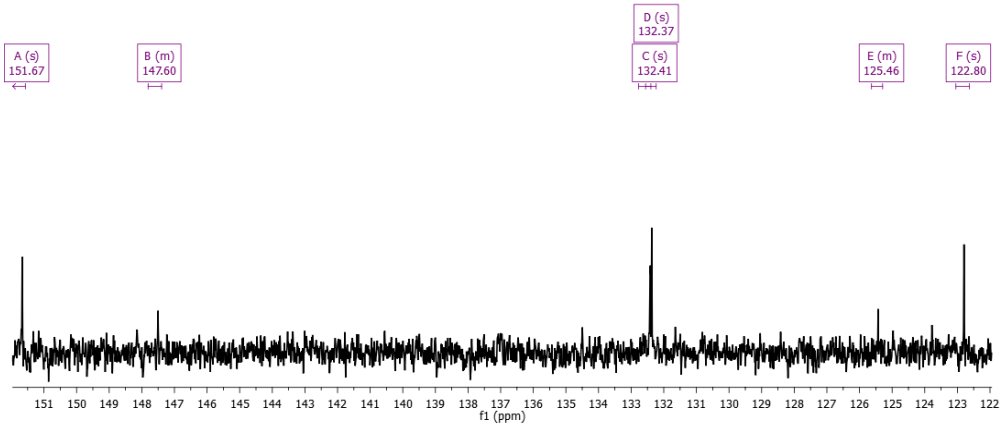

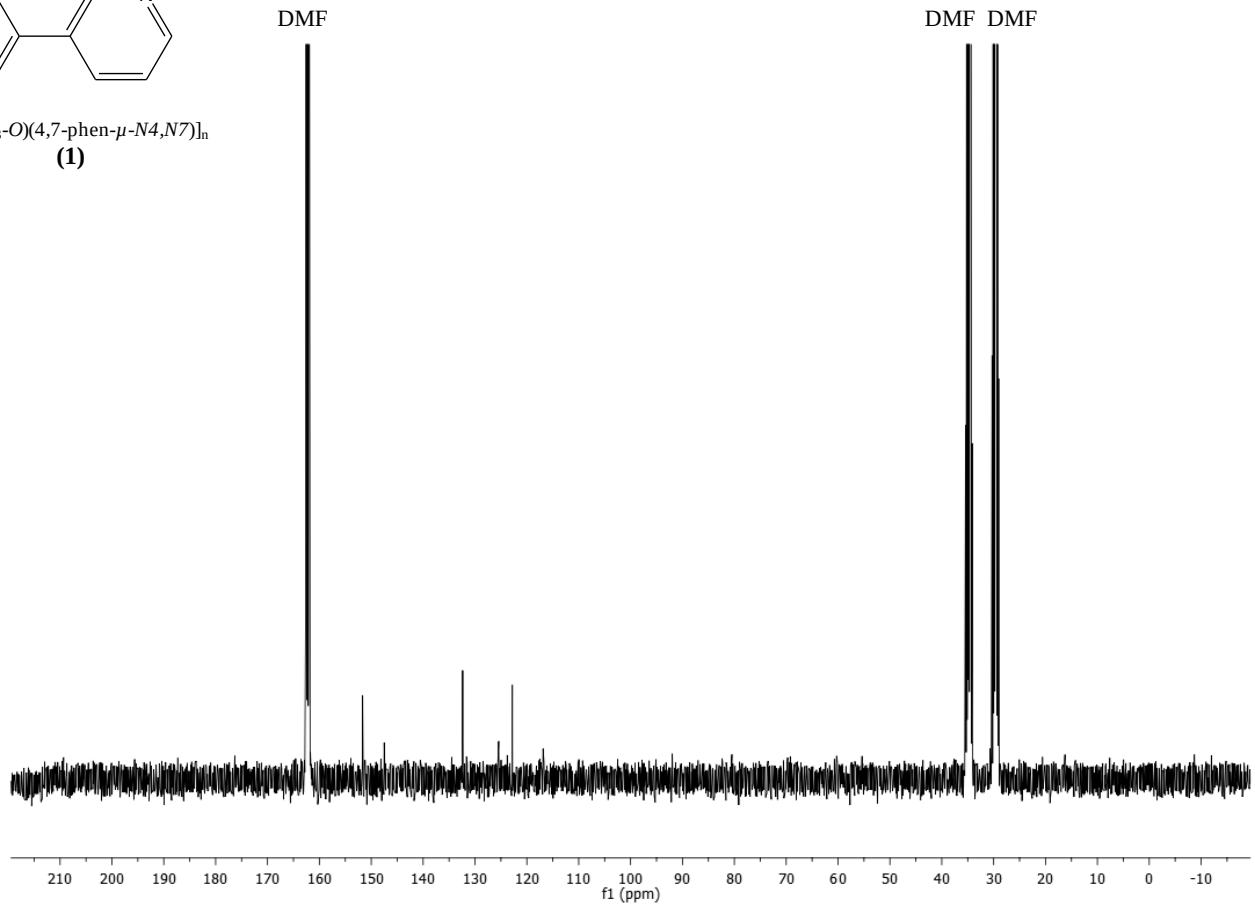

^{1}H NMR (400 MHz, DMF-d_7)

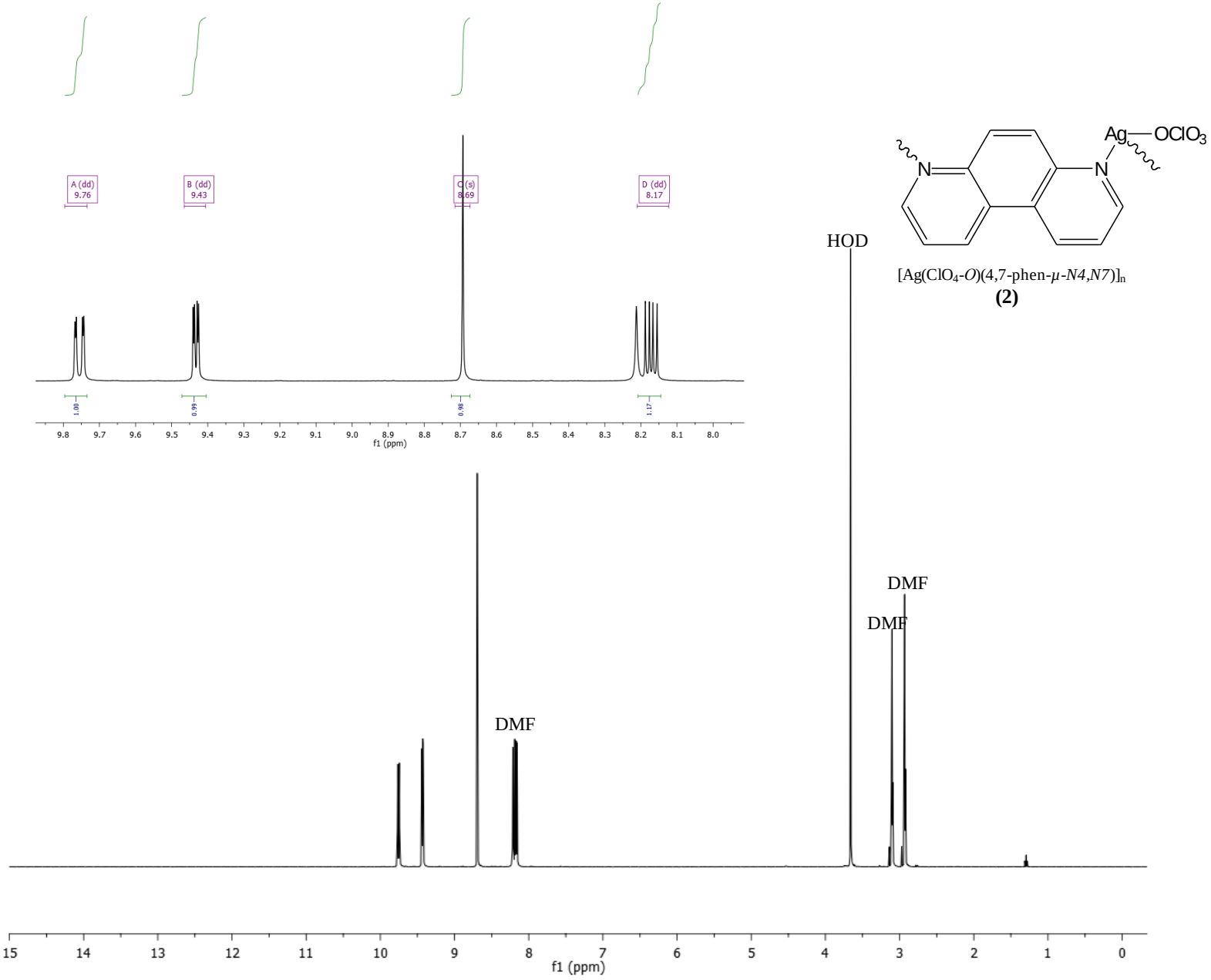

[Ag(ClO_4-*O*)(4,7-phen-*μ*-*N4*,*N7*)]$_n$

(2)

^{13}C NMR (101 MHz, DMF-d_7)

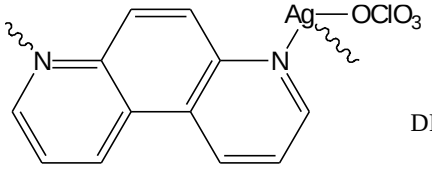

[Ag(ClO_4-*O*)(4,7-phen-μ-*N4*,*N7*)]$_n$

(2)

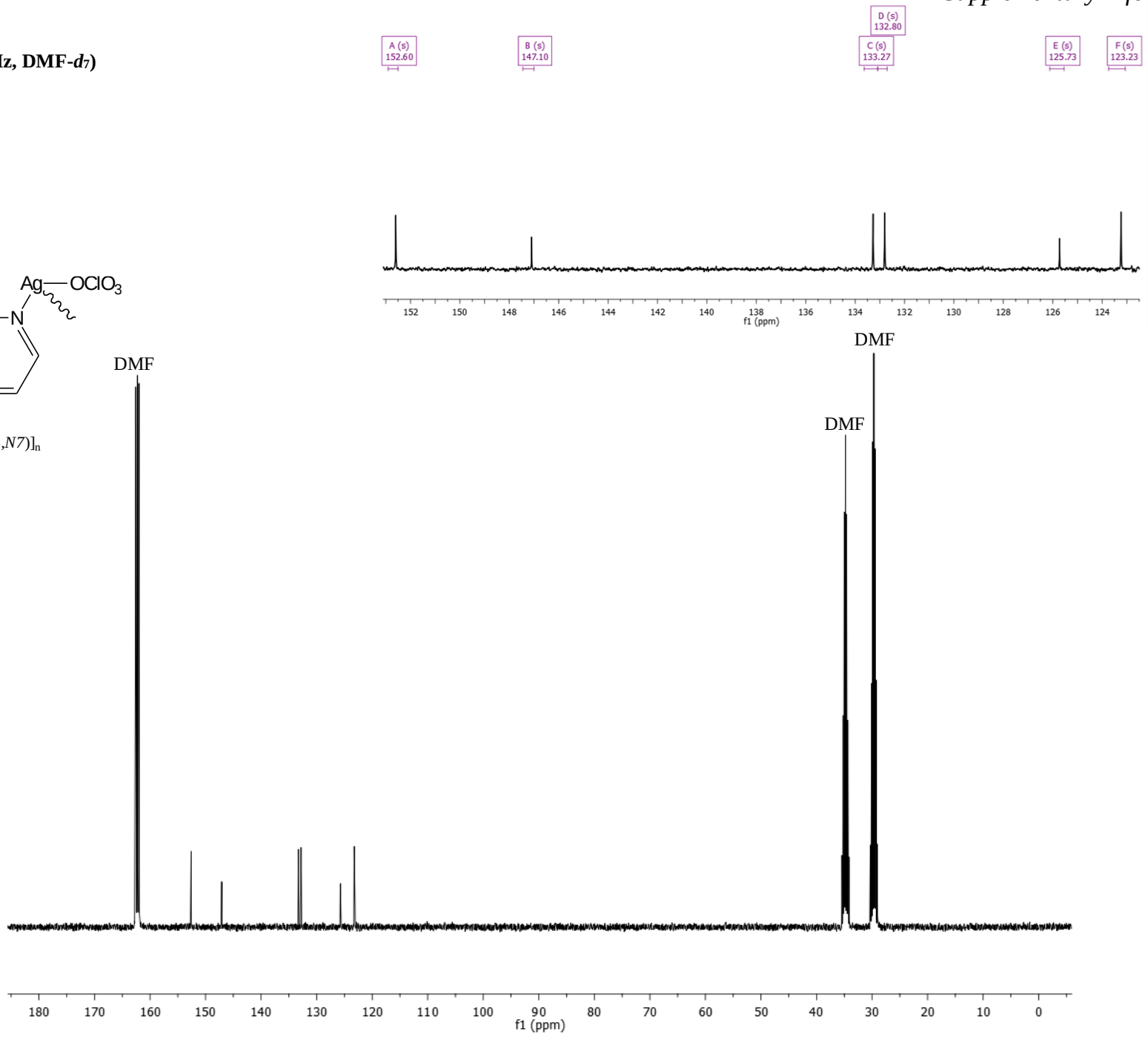

^{1}H NMR (400 MHz, DMF-d_7)

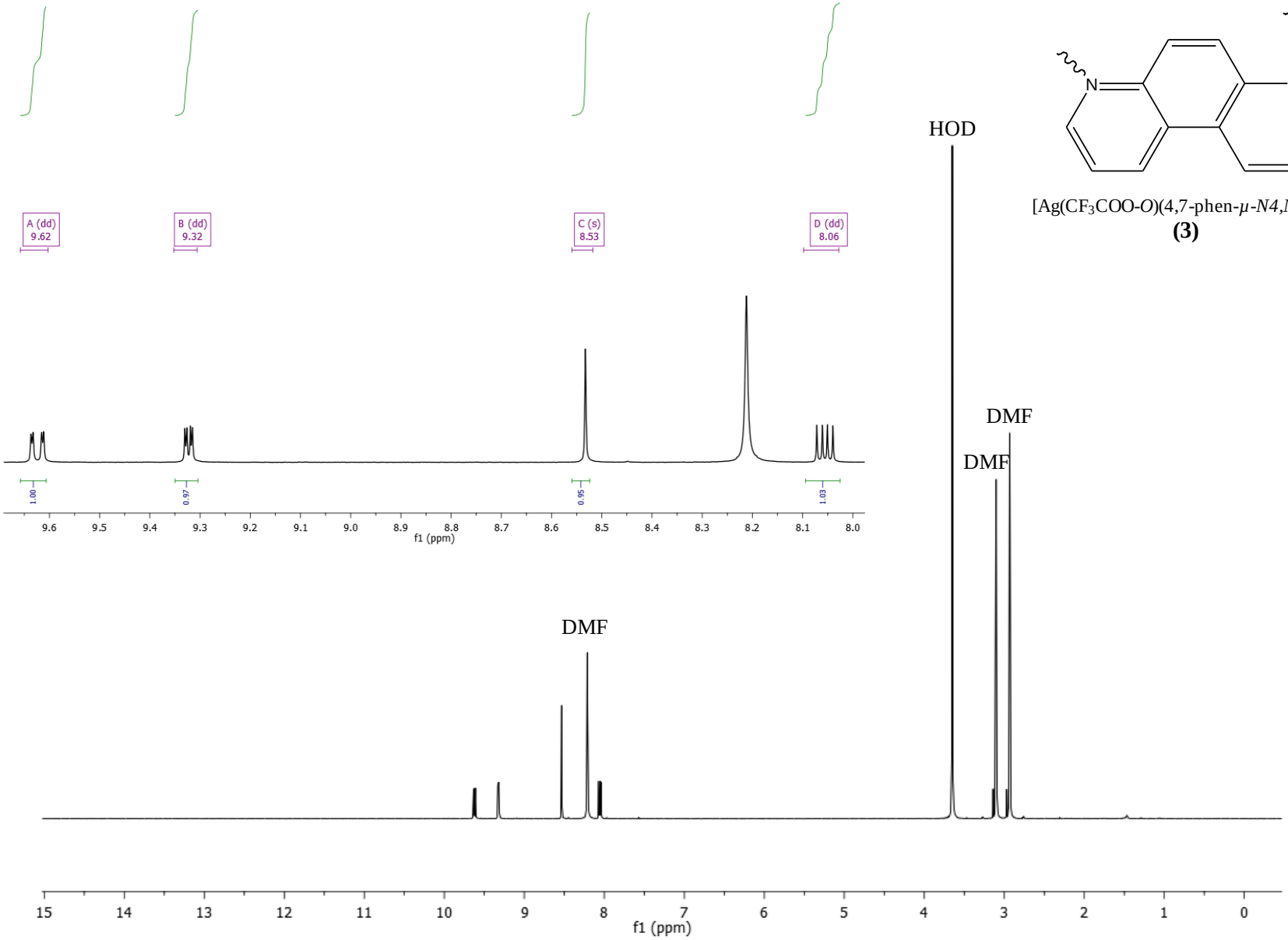

[Ag(CF$_3$COO-*O*)(4,7-phen-*μ*-*N4*,*N7*)]$_n$

(3)

^{13}C NMR (101 MHz, DMF-d_7)

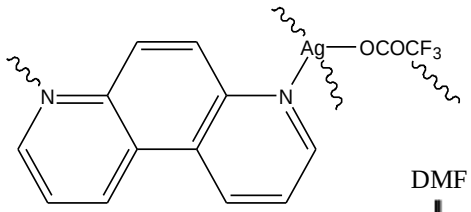

[Ag(CF_3COO-*O*)(4,7-phen-μ-*N4*,*N7*)]$_n$

(3)

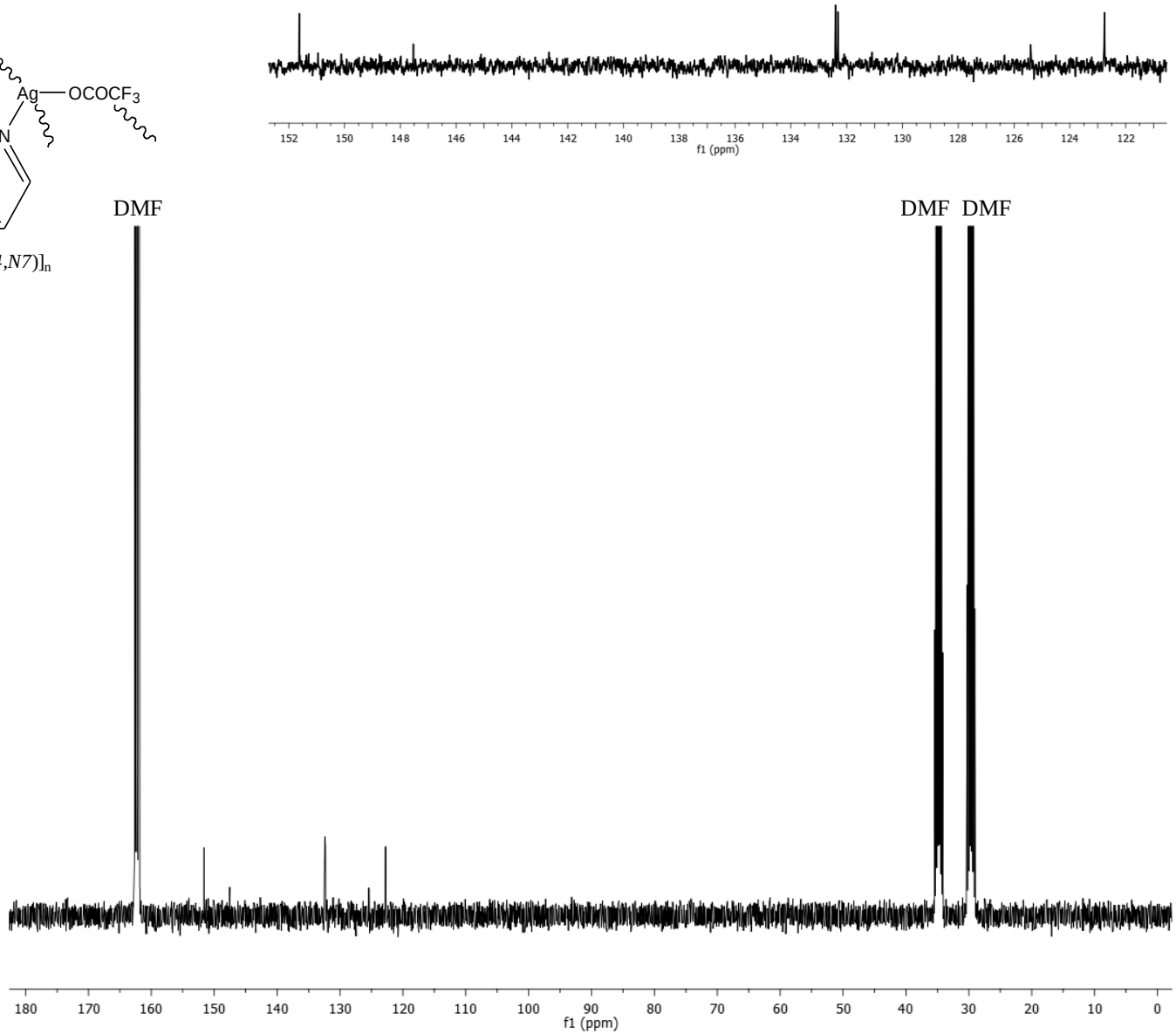

^{1}H NMR (400 MHz, DMF-d_7)

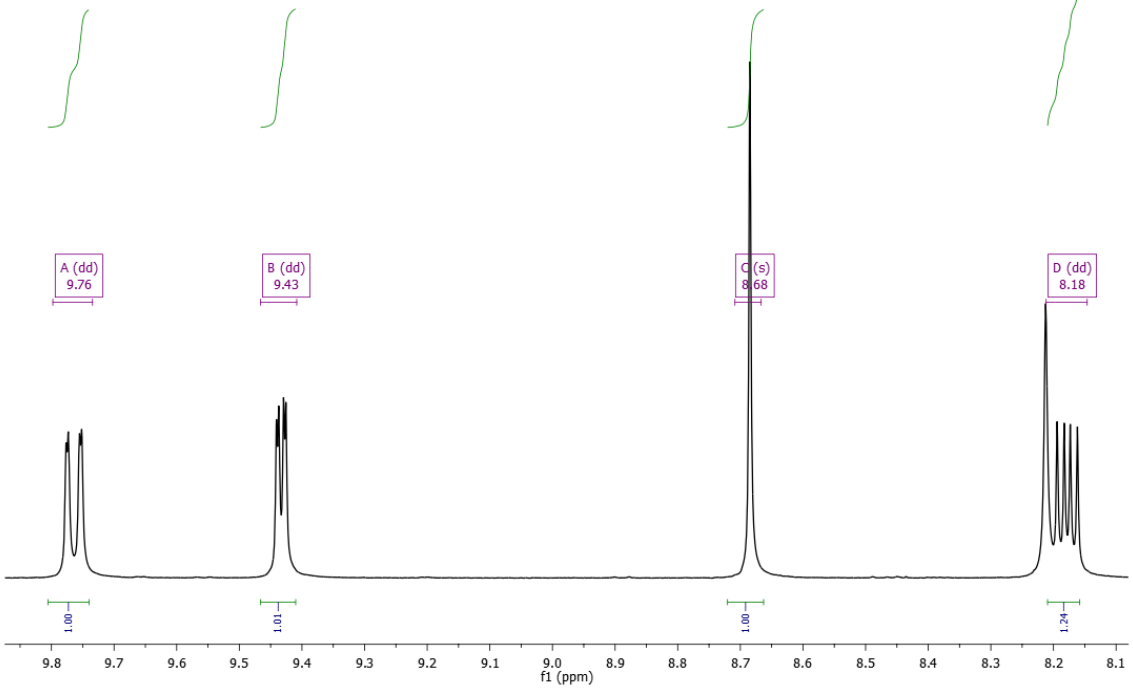

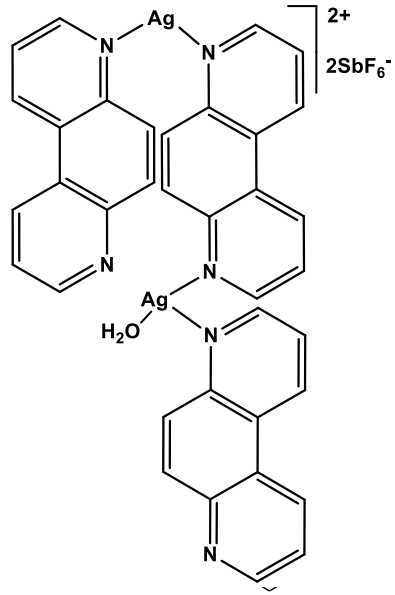

$[Ag_2(H_2O)_{0.58}(4,7\text{-phen})_3](SbF_6)_2$

(4)

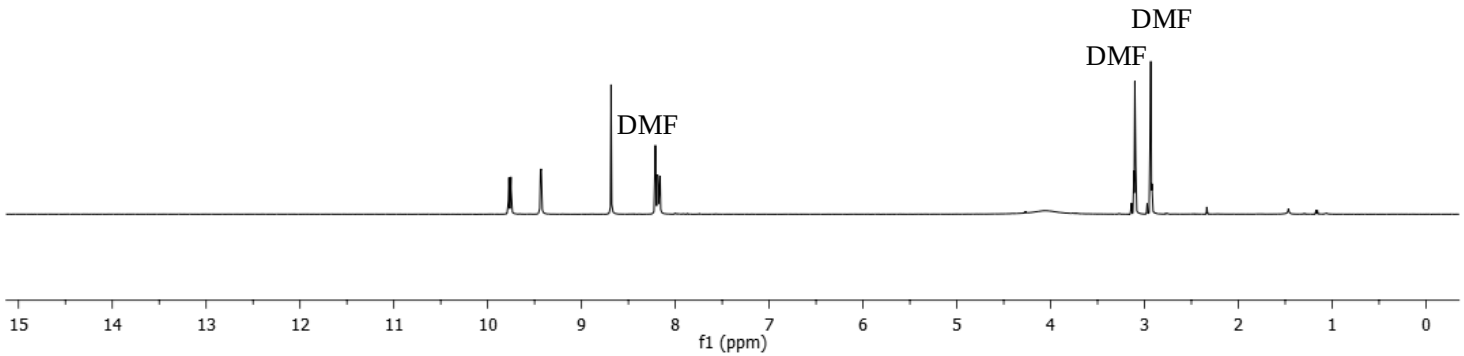

^{13}C NMR (101 MHz, DMF-d_7)

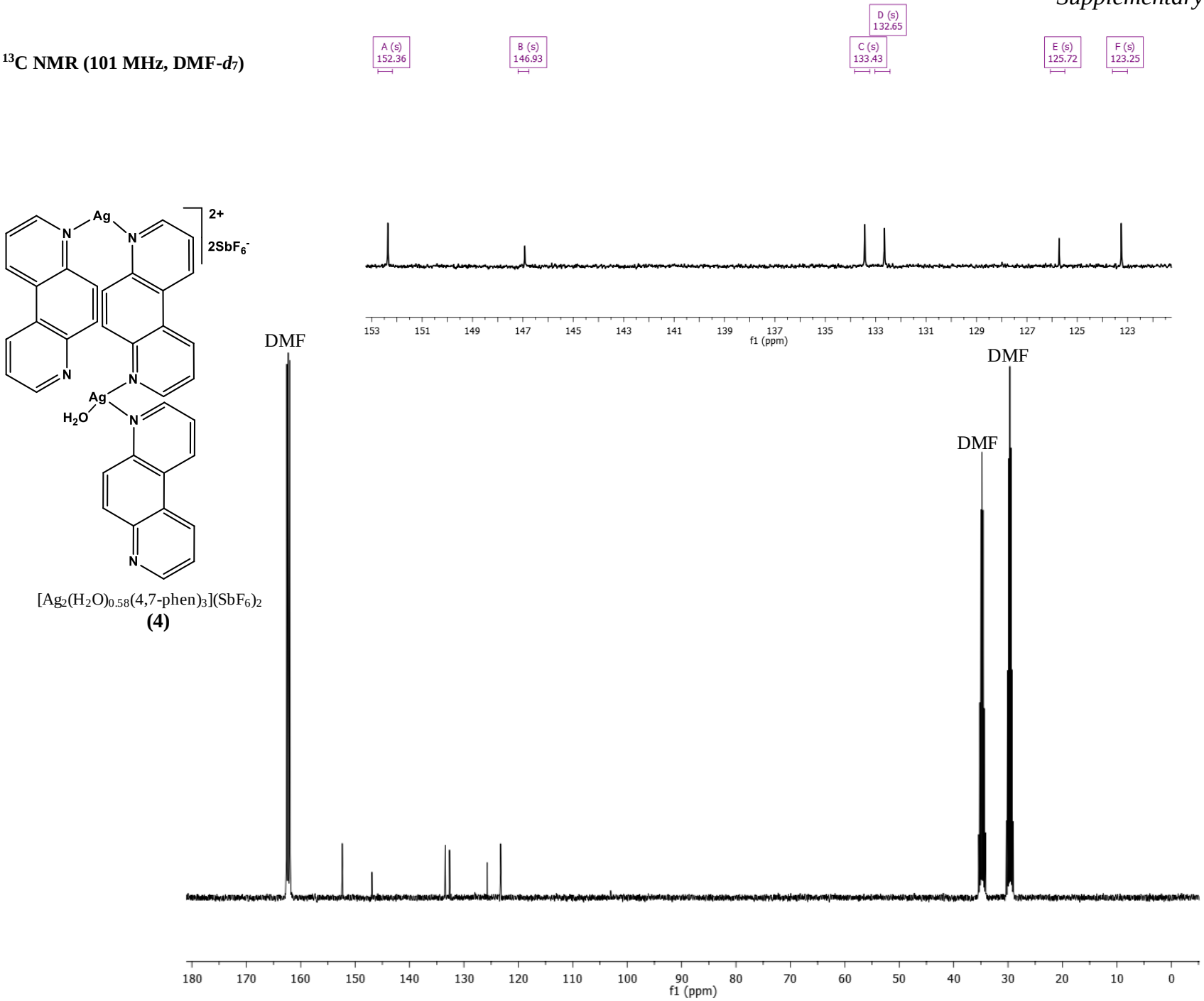

$[Ag_2(H_2O)_{0.58}(4,7\text{-phen})_3](SbF_6)_2$

(4)

^{1}H NMR (400 MHz, DMF-d_7)

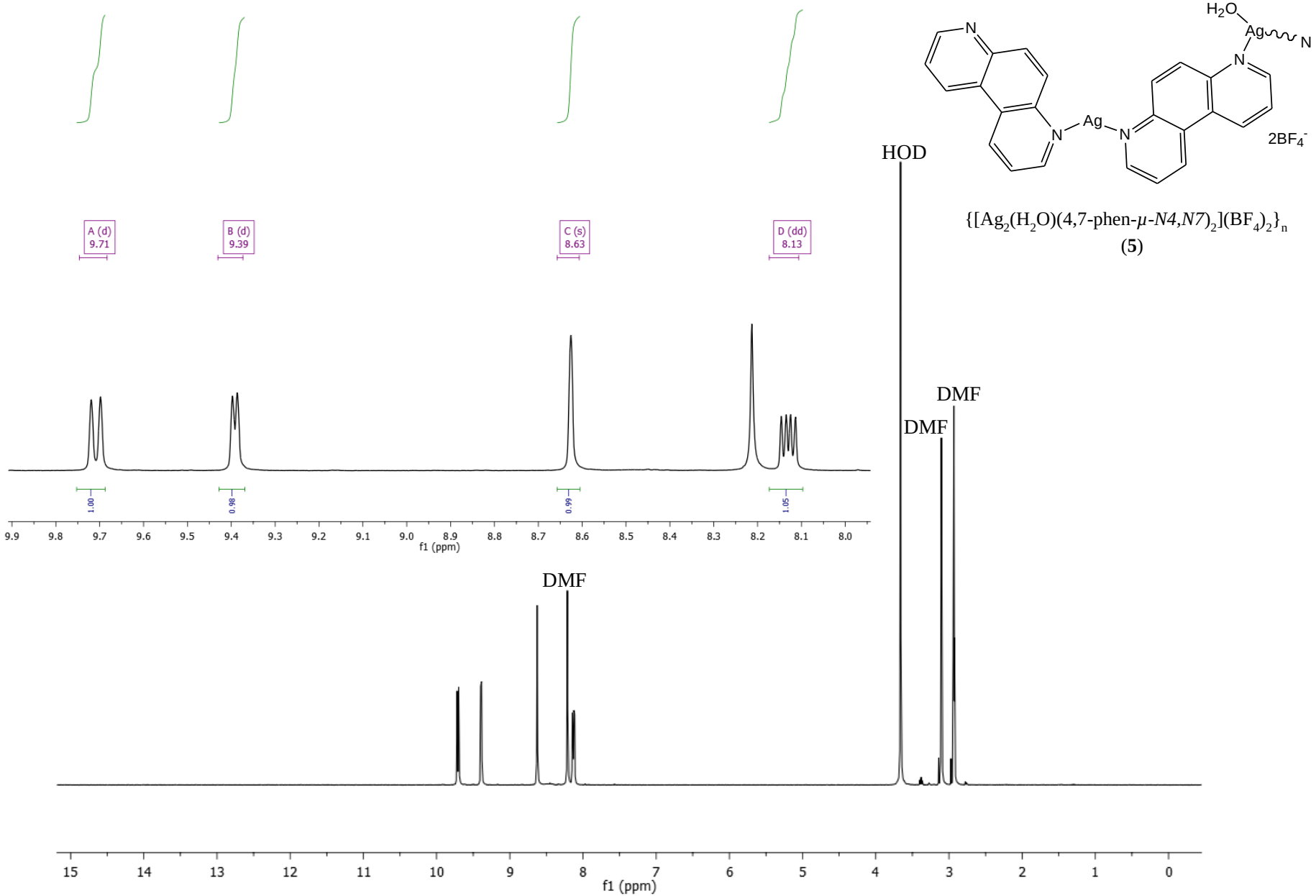

{[$Ag_2(H_2O)$(4,7-phen-μ-*N4,N7*)$_2$]$(BF_4)_2$}$_n$

(**5**)

^{13}C NMR (101 MHz, DMF-d_7)

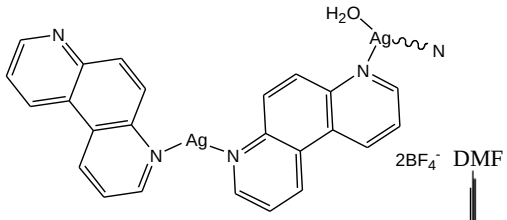

{[$Ag_2(H_2O)$(4,7-phen-μ-*N4*,*N7*)$_2$]$(BF_4)_2$}$_n$

(**5**)

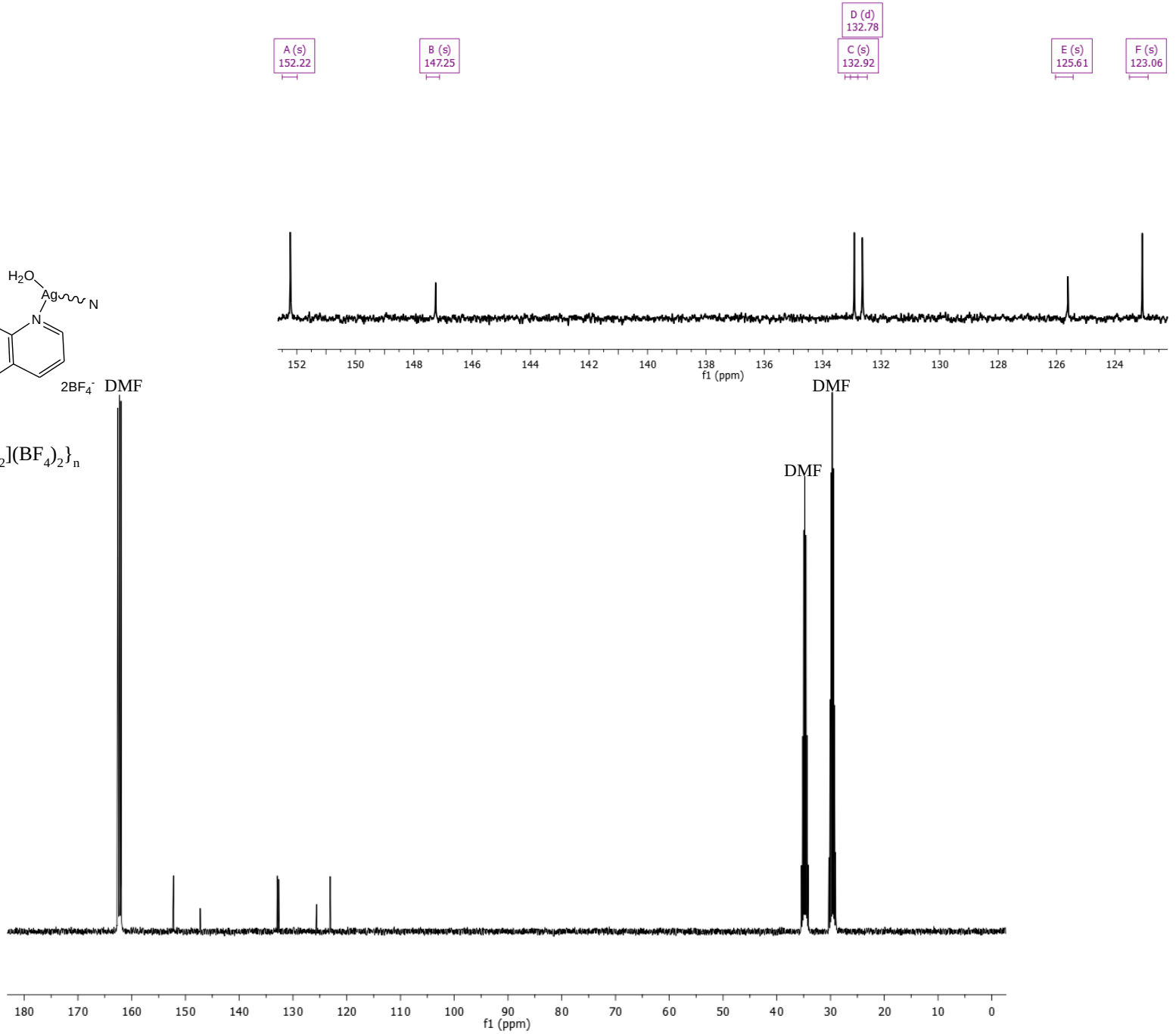

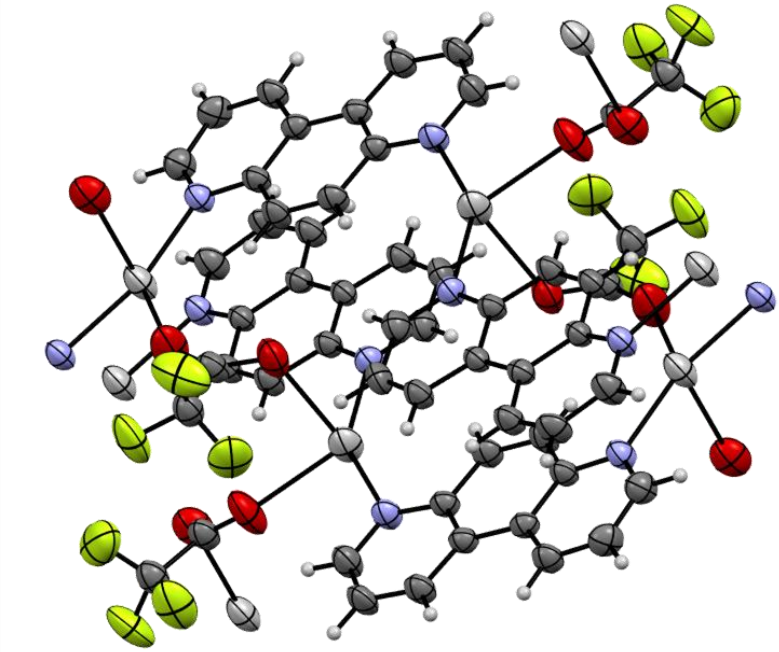

Fig. S1. An extended view of the polynuclear complex **3**.

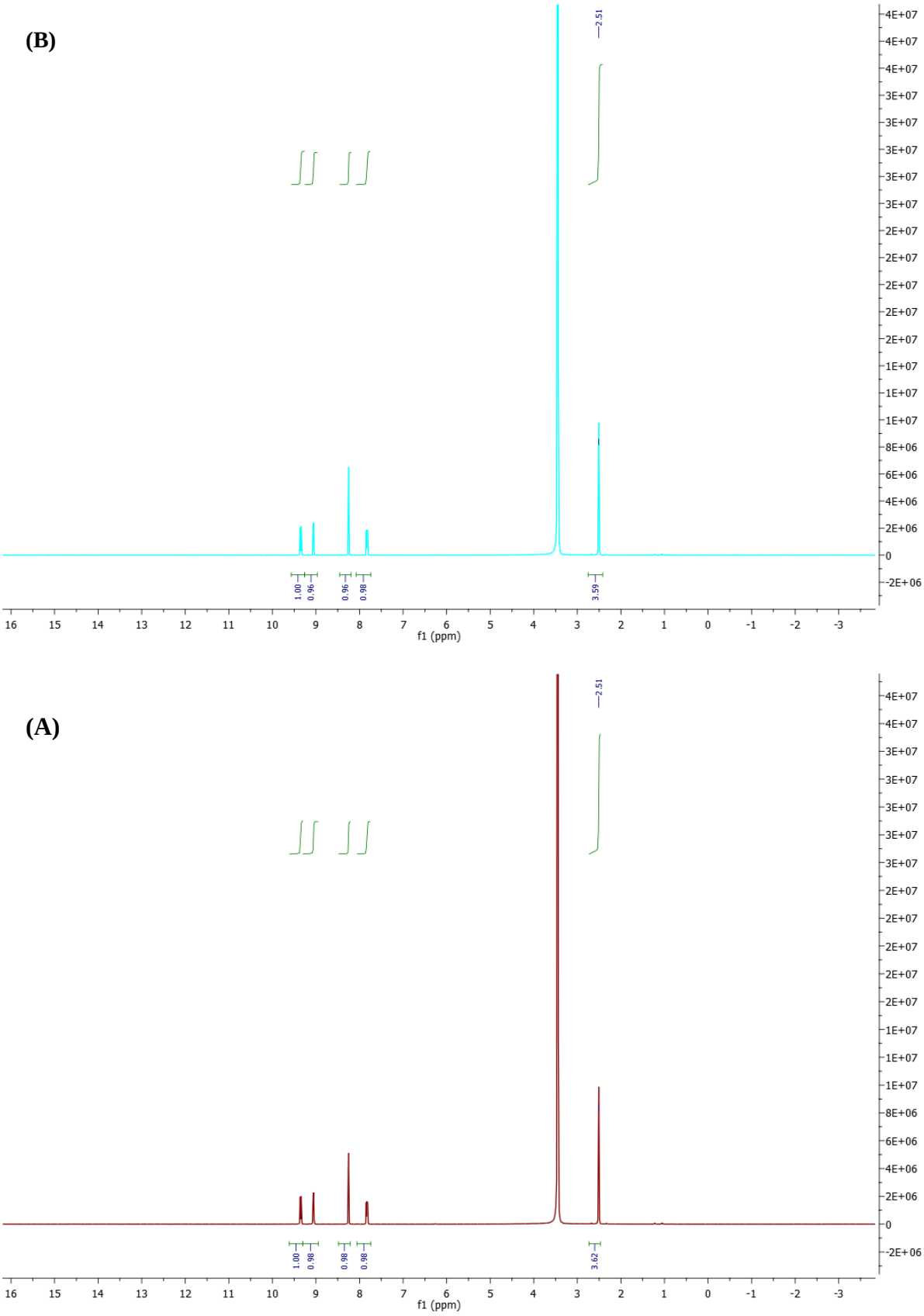

Fig. S2. Complex **4** stability over time measured by ^{1}H NMR spectroscopy. ^{1}H NMR spectrum was measured immediately (A) and 24 h (B) after complex dissolution in DMSO-d_6.

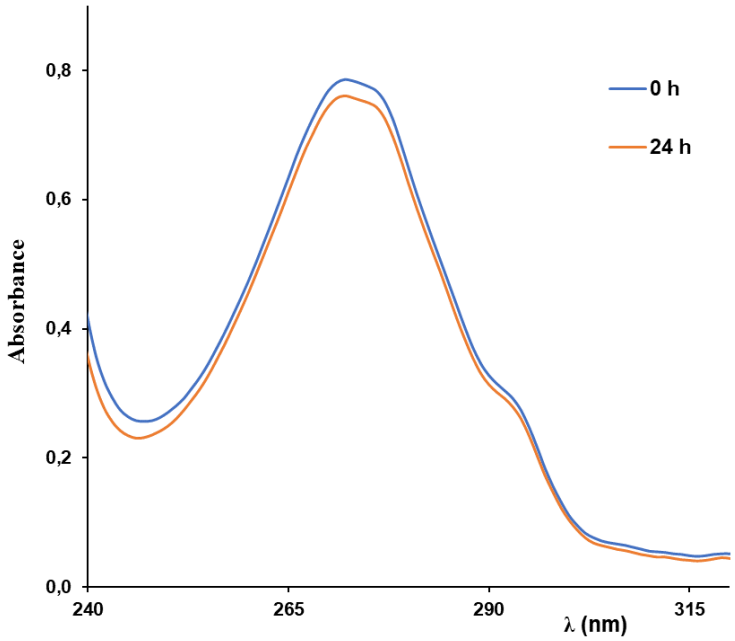

Fig. S3. Complex **4** stability over time followed by UV-Vis spectrophotometry in DMF/RPMI medium containing 2% of glucose.

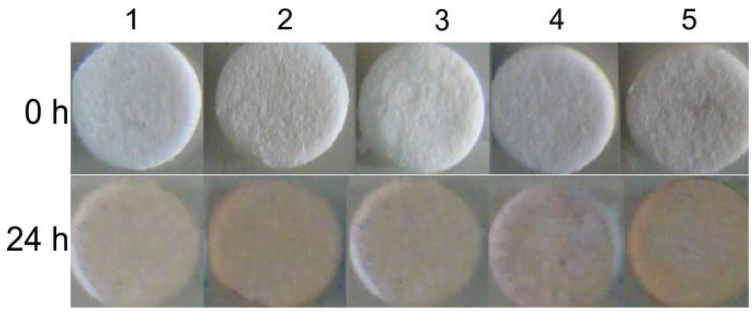

Fig. S4. The air/light stability of silver(I) complexes **1 – 5**.

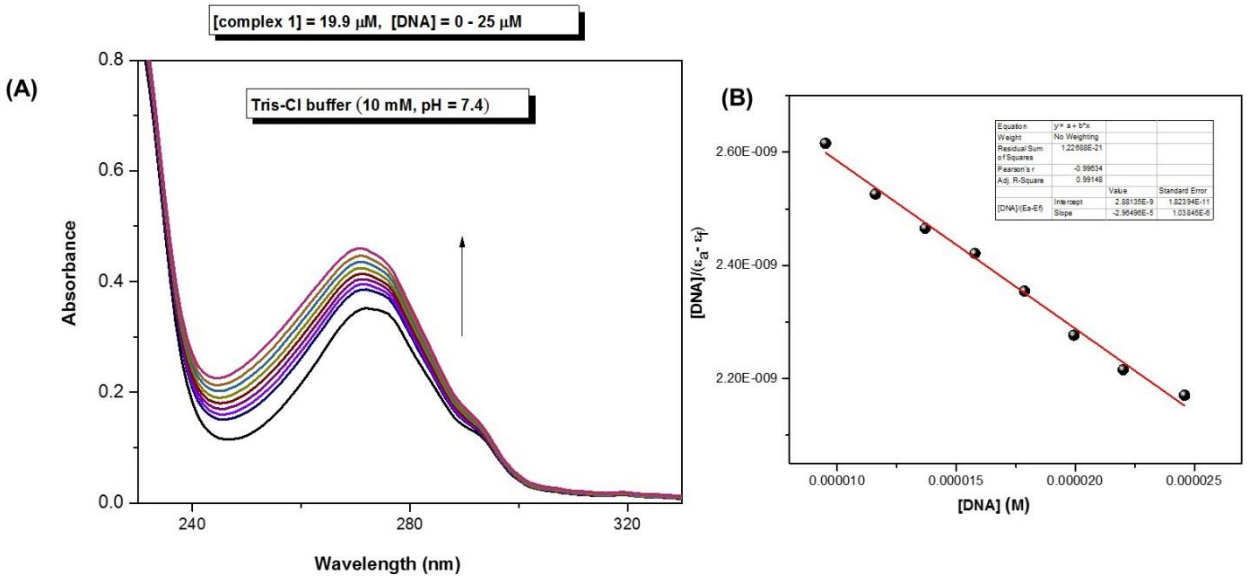
(A)
[complex 1] = 19.9 μM, [DNA] = 0 - 25 μM
Tris-Cl buffer (10 mM, pH = 7.4)
Absorbance
Wavelength (nm)
(B)
[DNA]/(εa - εf)
[DNA] (M)

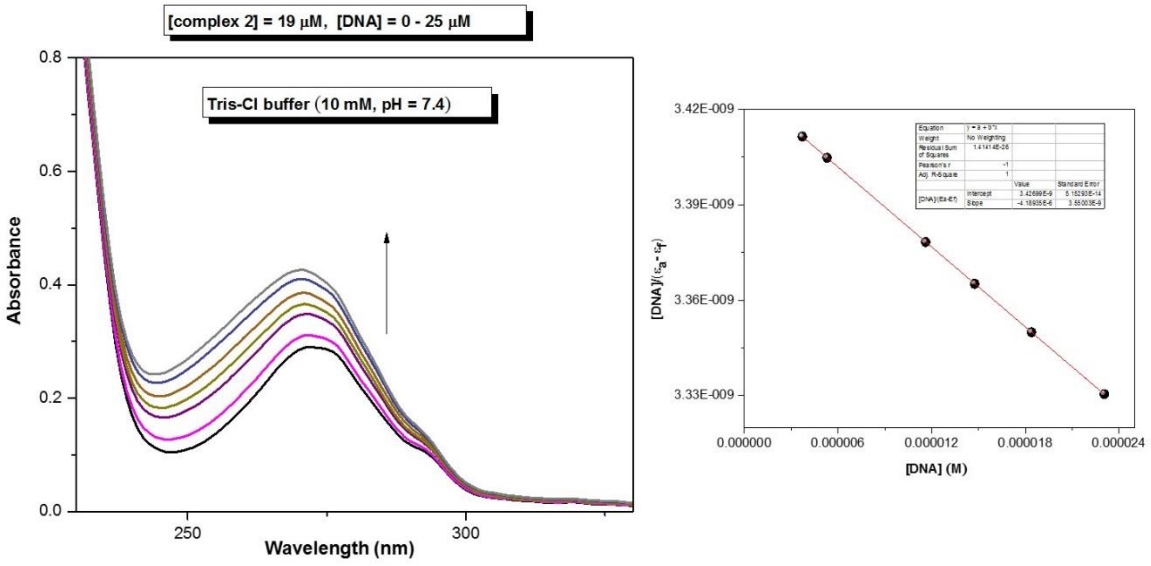
[complex 2] = 19 μM, [DNA] = 0 - 25 μM
Tris-Cl buffer (10 mM, pH = 7.4)
Absorbance
Wavelength (nm)
[DNA]/(εa - εf)
[DNA] (M)

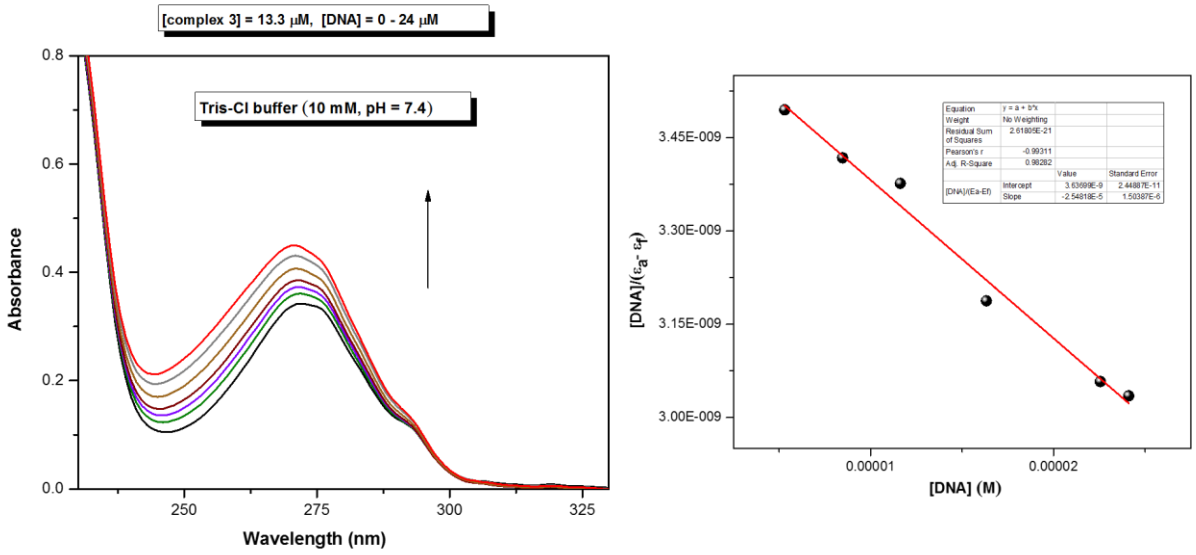
[complex 3] = 13.3 μM, [DNA] = 0 - 24 μM
Tris-Cl buffer (10 mM, pH = 7.4)
Absorbance
Wavelength (nm)
[DNA]/(εa - εf)
[DNA] (M)

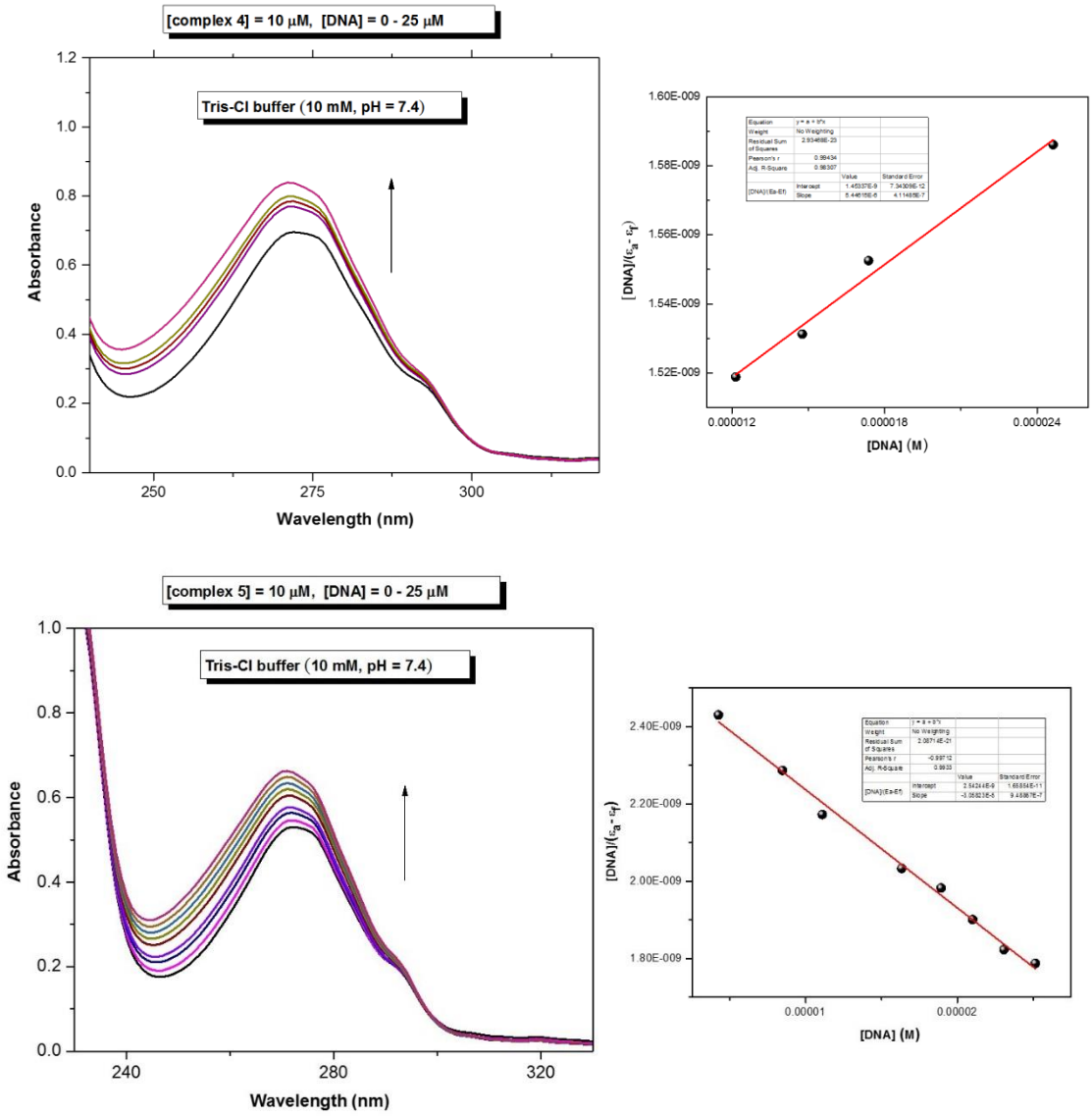

Fig. S5. (A) Absorption spectra of the silver(I) complexes **1 – 5** in Tris buffer upon addition of DNA. Arrow shows the change of absorbance upon increasing concentration of DNA. (B) Plot of [DNA]/($\varepsilon_a - \varepsilon_f$) versus [DNA].

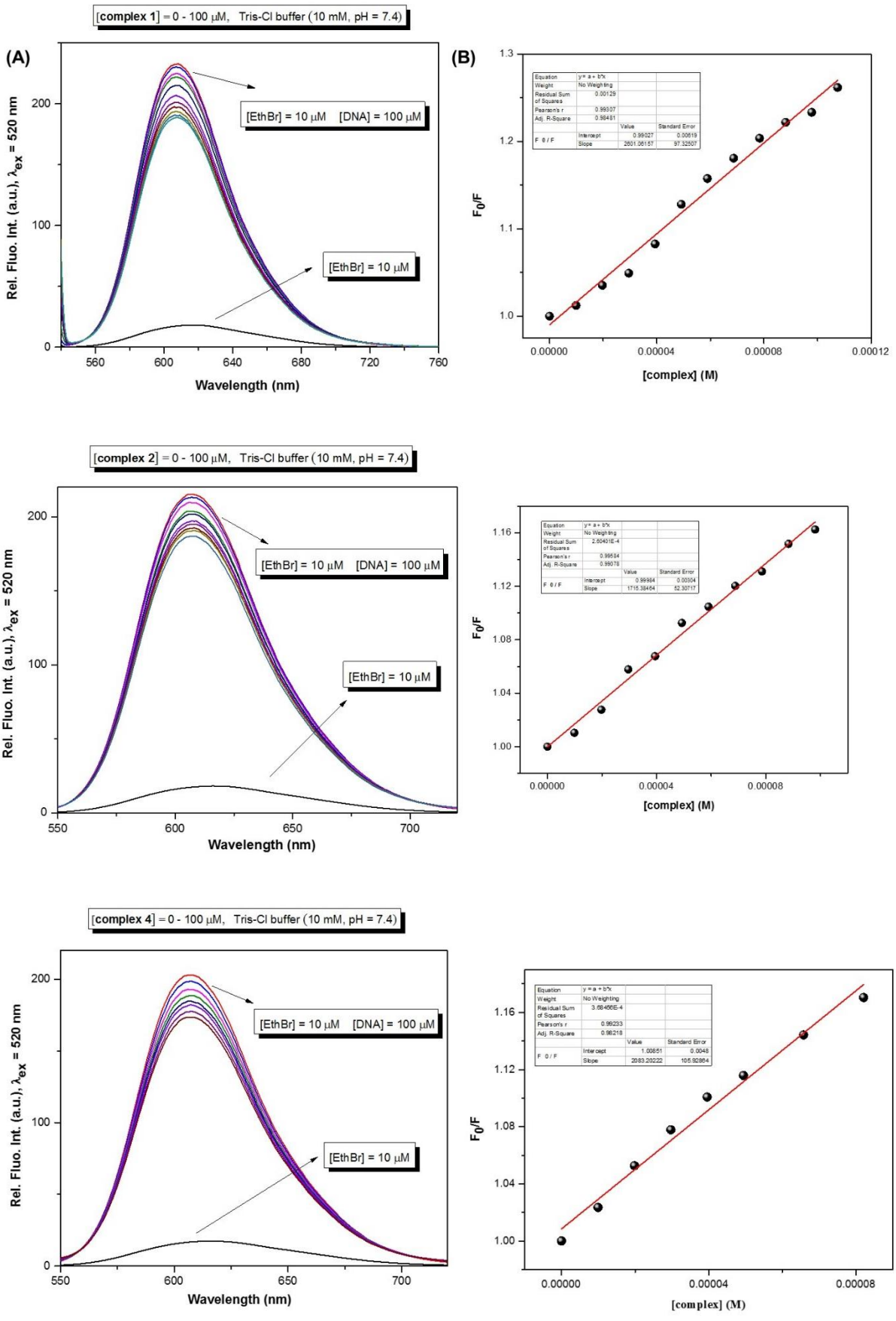
[complex 1] = 0 - 100 μM, Tris-Cl buffer (10 mM, pH = 7.4)
(A)
[EthBr] = 10 μM [DNA] = 100 μM
[EthBr] = 10 μM
Rel. Fluo. Int. (a.u.), λex = 520 nm
Wavelength (nm)
(B)
F0/F
[complex] (M)
[complex 2] = 0 - 100 μM, Tris-Cl buffer (10 mM, pH = 7.4)
[EthBr] = 10 μM [DNA] = 100 μM
[EthBr] = 10 μM
Rel. Fluo. Int. (a.u.), λex = 520 nm
Wavelength (nm)
F0/F
[complex] (M)
[complex 4] = 0 - 100 μM, Tris-Cl buffer (10 mM, pH = 7.4)
[EthBr] = 10 μM [DNA] = 100 μM
[EthBr] = 10 μM
Rel. Fluo. Int. (a.u.), λex = 520 nm
Wavelength (nm)
F0/F
[complex] (M)

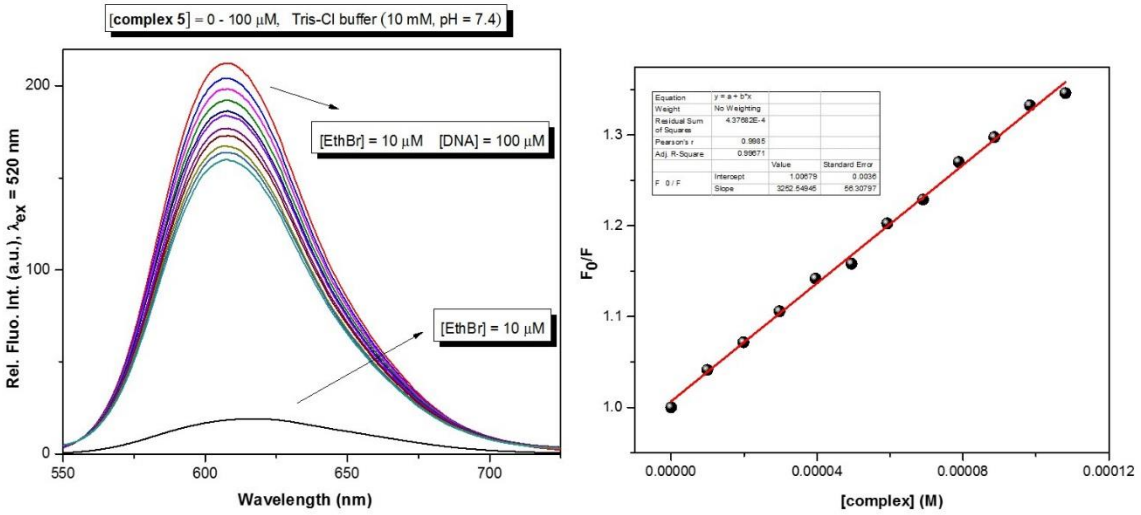

Fig. S6. (A) Fluorescence emission spectra of EthBr bound to DNA in the absence and presence of the silver(I) complexes in Tris buffer at 25 ^{o}C. Arrow shows the change upon increasing concentration of complex. (B) Stern-Volmer plots of relative EthBr-DNA fluorescence intensity F_0/F *vs* [complex].

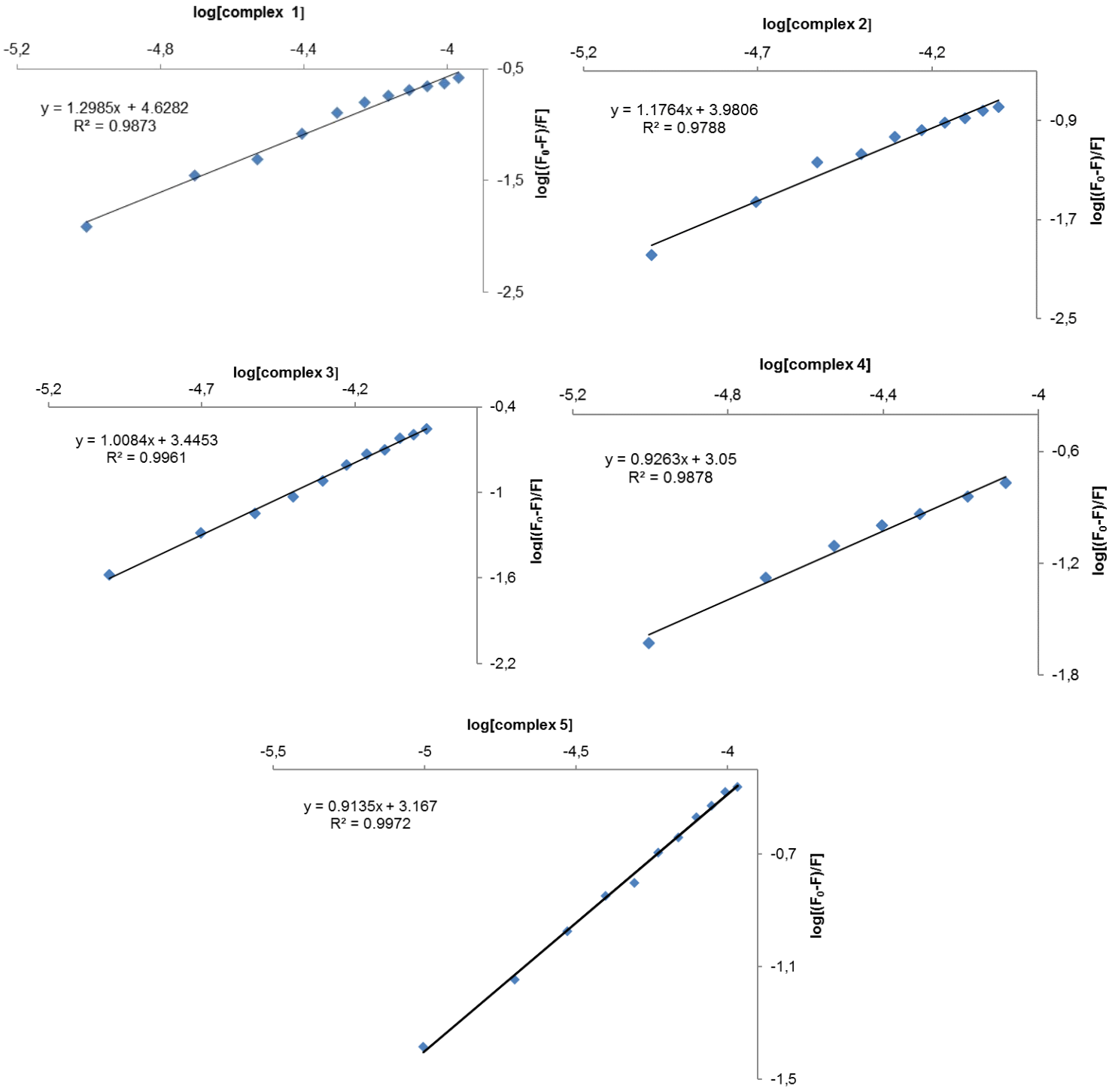

Fig. S7. Plot of $\log(F_0 - F)/F$ *vs* log[complex].

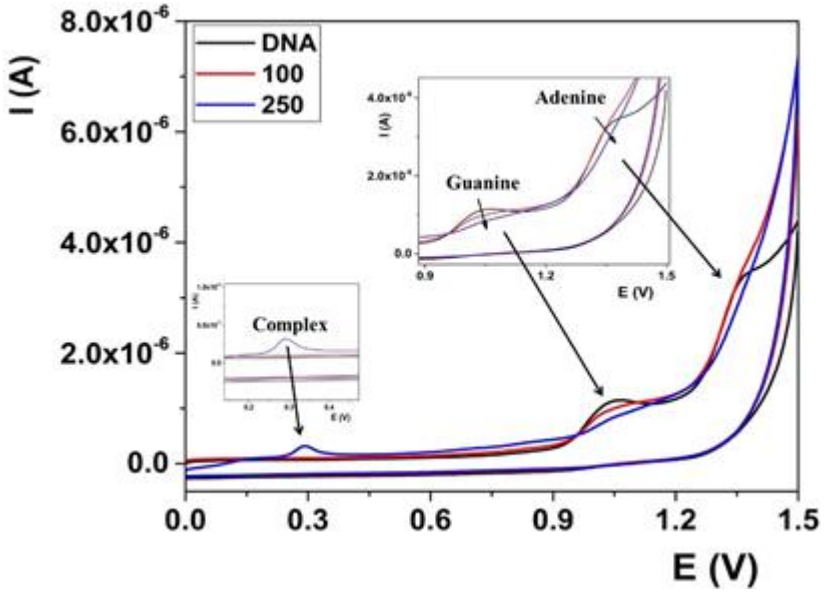

Fig. S8. CV voltammograms of DNA after addition of complex **4** in the concentrations range from 0 to 250 ppm.

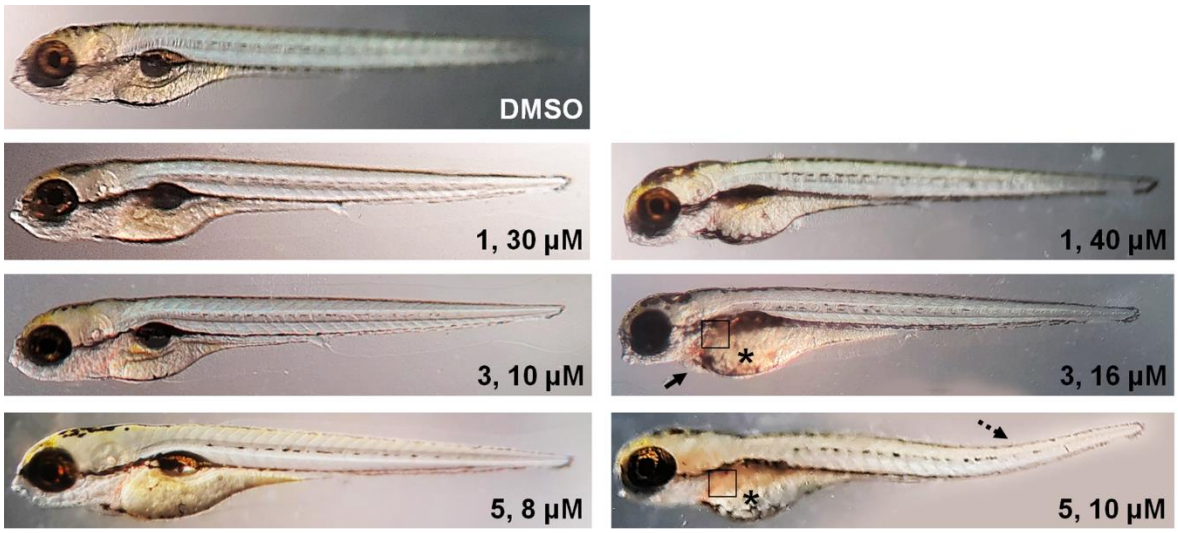

Fig. S9. Toxicity evaluation of silver(I) complexes **1**, **3** and **5** in the zebrafish model. The normally developed fish are shown on the left panel of photos including the control one (DMSO-treated), while the affected (teratogenic) fish are shown on the right panel. In comparison to the untreated fish, the teratogenic fish upon complexes showed signs of weak hepatotoxicity – slightly darker liver (boxed area), weakly absorbed the yolk (asterics) and shorter body, had weak pericardial edema (arrow) and lordosys (dashed arrea).

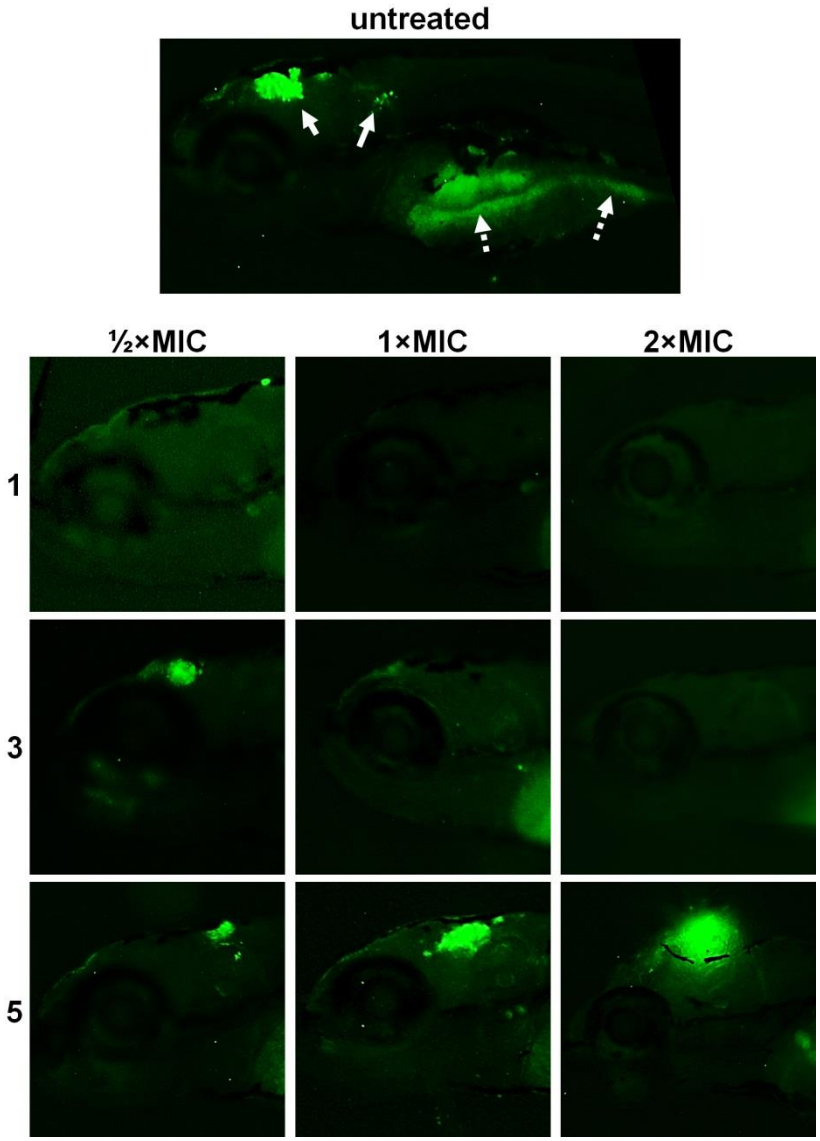

Fig. S10. Eradication of *C. albicans* infection from the body of zebrafish larvae after the 3 days treatments with different doses (½×MIC, 1×MIC and 2×MIC) of silver(I) complexes **1**, **3** and **5**. In the untreated embryos at 3 dpi (120 hpf), fungal infection has mainly been localized in the head (arrow) and the intestine (dashed arrow). Complexes **1** and **3** successfully inhibited fungal filamentation by 4 dpi at any applied dose, while the treatment with **5** resulted in the filamentation increase with complex's concentration increase.

Table S1

Details of the crystal structure determinations of the silver(I) complexes **1 – 5**.

	1	**2**	**3**	**4**	**5**
Empirical formula	$C_{12}H_8AgN_3O_3$	$C_{12}H_8AgClN_2O_4$	$C_{14}H_8AgF_3N_2O_2$	$C_{36}H_{25.15}Ag_2F_{12}N_6O_{0.58}Sb_2$	$C_{24}H_{18}Ag_2B_2F_8N_4O$
CCDC number	1879001	1879002	1879003	1879004	1880758
Formula weight (g/mol)	350.08	387.52	401.09	1238.21	767.78
Crystal system, space group	monoclinic, $P2_1/c$	monoclinic, $P2_1/c$	monoclinic, $P2_1/c$	triclinic, $P\bar{1}$	triclinic, $P\bar{1}$
a (Å)	10.7794(15)	10.2659(6)	11.7244(14)	10.7878(8)	7.1974(4)
b (Å)	14.485(2)	14.6602(11)	14.7916(16)	12.1188(8)	11.8682(6)
c (Å)	7.320(2)	7.9925(7)	7.4544(9)	14.5250(10)	15.0708(8)
α (°)				82.918(5)	79.146(4)
β (°)	100.585(17)	97.922(6)	95.644(10)	88.316(6)	76.397(4)
γ (°)				85.176(6)	82.976(4)
V (Å^3)	1123.5(4)	1191.39(15)	1286.5(3)	1877.4(2)	1224.75(12)
F_{000}	688	760	784	1184	748
Z	4	4	4	2	2
X-radiation, λ /Å	Mo-K_α 0.71073	Mo-K_α 0.71073	Mo-K_α 0.71073	Mo-K_α 0.71073	Mo-K_α 0.71073
data collect. temperat. /K	298(2)	250(2)	298(2)	250(2)	200(2)
Calculated density (Mg/m^3)	2.070	2.160	2.071	2.190	2.082
Absorption coefficient (mm^{-1})	1.801	1.931	1.612	2.551	1.689
Crystal size (mm^3)	0.64 × 0.26 × 0.02	0.38 x 0.167 x 0.04	0.39 × 0.17 × 0.05	0.37 × 0.183 × 0.07	0.30 × 0.15 × 0.06
2θ range (°)	3.8 to 50.5	4.0 to 50.5	3.4 to 50.6	2.8 to 50.5	3.5 to 50.2
index ranges h, k, l	-12 ... 12, -17 ... 17, -8 ... 8	-12 … 12, -17… 17, -9 ... 9	-14 ... 13, -17 ... 17, -8 ... 8	-12 ... 12, -14 ... 14, -17 ... 17	-8 ... 8, -14 ... 14, -17 ... 17
No. of collected and independent reflections	12782, 2013	12271, 2126	16077, 2296	6286, 6286	13046, 4351
R_{int}	0.0684	0.0371	0.1070		0.0391
Data / restraints / parameters	2013 / 0 / 172	2126 / 0 / 181	2296 / 0 /199	6286 / 57 / 408	4351 / 3 / 376
Goodness-on-fit on F^2	1.040	1.034	1.055	1.041	1.045
Final R indices $[I \geq 2\sigma(I)]$	0.0362, 0.0727	0.0232, 0.0546	0.0346, 0.0800	0.0929, 0.2586	0.0237, 0.0628
Final R indices (all data)	0.0543, 0.0779	0.0348, 0.0579	0.0497, 0.0888	0.1125, 0.2837	0.0268, 0.0645
Difference density: max, min (e/Å^3)	0.75, -0.34	0.32, -0.34	0.70, -0.61	2.01, -2.11	0.56, -0.46

Table S2

Lethal and teratogenic effects observed in zebrafish (*Danio rerio*) embryos at different hours post fertilization (hpf).

Category	Developmental endpoints	Exposure time (hpf)			
		48	72	96	120
Lethal effect	Coagulated eggs	•	•	•	•
	Lack of the heart beating	•	•	•	•
Teratogenic effect	Malformation of head	•	•	•	•
	Malformation of eyes	•	•	•	•
	Malformation of sacculi/otoliths	•	•	•	•
	Malformation of chorda	•	•	•	•
	Malformation of tail	•	•	•	•
	Scoliosis	•	•	•	•
	Yolk edema	•	•	•	•
	Yolk deformation	•	•	•	•
	Growth retardation		•	•	•
	Hatching			•	•
Cardiotoxicity	Pericardial edema		•	•	•
	Heart morphology			•	•
	Heart beating rate (beat/min)				•

[a]No clear organs structure is recognized.
[b]Malformation of eyes was recorded for the retardation in eye development and abnormality in shape and size.
[c]Presence of none, one or more than two otoliths per sacculus, as well as reduction and enlargement of otoliths and/or sacculi (otic vesicles).
[d]Tail malformation was recorded when the tail was bent, twisted or shorter than to control embryos as assessed by optical comparation.
[e]Growth retardation was recorded by comparing with the control embryos in a body length (after hatching, at and onwards 72 hpf) using by optical comparation using an inverted microscope (CKX41; Olympus, Tokyo, Japan).

Table S3

Selected bond distances (Å) and valence angles (°) in silver(I) complexes **1** – **5**.

1		**2**		**3**		**4**		**5**	
Ag1—N1	2.274(3)	Ag1—N1	2.196(2)	Ag1—N1	2.239(3)	Ag1—N3	2.111(15)	Ag1—N3	2.168(2)
Ag1—N2	2.268(3)	Ag1—N2^{i}	2.193(2)	Ag1—N2	2.254(3)	Ag1—N2	2.102(13)	Ag1—N1	2.170(2)
Ag1—O3	2.544(4)	Ag1—O1	2.571(2)	Ag1—O1	2.440(3)	Ag2—O1	2.43(2)	Ag2—N4	2.161(2)
Ag1—O1	3.495(5)			Ag1—O2^{iii}	2.635(4)	Ag2—N4	2.135(14)	Ag2—N2^{iv}	2.171(2)
Ag1—O2’	2.739(6)					Ag2—N5	2.155(11)	Ag2—O1	2.631(2)
Ag1—O3’	2.759(6)								
N1—Ag1—N2	139.34(12)	N2^{i}—Ag1—N1	150.98(9)	N1—Ag1—N2	144.95(12)	N2—Ag1—N3	175.4(5)	N1—Ag1—N3	165.01(8)
N1—Ag1—O3	113.16(12)	N2^{i}—Ag1—O1	110.70(9)	N1—Ag1—O1	124.22(12)	N4—Ag2—O1	93.8(6)	N2^{iv}—Ag2—N4	162.57(8)
N2—Ag1—O3	92.34(13)	N1—Ag1—O1	86.10(9)	N2—Ag1—O1	89.78(12)	N4—Ag2—N5	167.7(5)	C1—N1—Ag1	119.40(17)
C1—N1—Ag1	120.9(3)	C1—N1—Ag1	120.2(2)	N1—Ag1—O2^{iii}	84.49(11)	N5—Ag2—O1	98.5(6)	C5—N1—Ag1	121.88(16)
C5—N1—Ag1	121.4(2)	C5—N1—Ag1	120.44(18)	N2—Ag1—O2^{iii}	107.51(12)	C13—N3—Ag1	121.0(10)	C12—N2—Ag2^{v}	121.07(19)
C12—N2—Ag1	119.2(3)	C12—N2—Ag1^{ii}	120.3(2)	O1—Ag1—O2^{iii}	87.43(13)	C17—N3—Ag1	122.1(12)	C8—N2—Ag2^{v}	120.30(17)
C8—N2—Ag1	121.3(3)	C8—N2—Ag1^{ii}	121.67(19)	C1—N1—Ag1	120.5(3)	C12—N2—Ag1	119.2(11)	C13—N3—Ag1	118.75(18)
N3—O3—Ag1	123.2(3)	Cl1—O1—Ag1	125.91(14)	C5—N1—Ag1	121.1(2)	C8—N2—Ag1	124.1(11)	C17—N3—Ag1	122.34(16)
				C12—N2—Ag1	117.6(3)	C20—N4—Ag2	124.5(12)	C24—N4—Ag2	120.67(18)
				C8—N2—Ag1	123.2(2)	C24—N4—Ag2	119.4(10)	C20—N4—Ag2	120.59(16)
				C25—O1—Ag1	147.4(3)	C25—N5—Ag2	118.9(10)		
				C25—O2^{iii}—Ag1	117.1(3)	C29—N5—Ag2	123.1(10)		
BVS_{Ag1}	0.97	BVS_{Ag1}	1.32	BVS_{Ag1}	1.01	BVS_{Ag1}	0.97	BVS_{Ag1}	0.84
						BVS_{Ag2}	1.13	BVS_{Ag2}	1.39

Symmetry code(s): (i) -*x*+1, *y*+1/2, -*z*+3/2; (ii) -*x*+1, *y*-1/2, -*z*+3/2; (iii) *x*, -*y*+1/2, *z*+1/2 (iv) *x*-1, *y*, *z*+1; (v) *x*+1, *y*, *z*-1

Table S4

Hydrogen bond parameters for silver(I) complexes **4** and **5**.

	D–H [Å]	D···A [Å]	H···A [Å]	D-H···A [°]	Symmetry codes
4					
O1–H1A···N1	0.87(2)	2.66(3)	1.944(17)	139.4(18)	*+x, +y, -1+z*
O1–H1B···N1	0.91(2)	3.16(3)	2.360(19)	147.1(19)	*1-x, 2-y, 2-z*
5					
O1–H1B···F7	0.832(18)	2.897(3)	2.12(2)	155(3)	*2-x, 1-y, 1-z*
O1–H1B···F5	0.832(18)	3.054(3)	2.34(3)	144(3)	*x+1, y, z-1*
O1–H1A···F3	0.826(18)	2.753(3)	1.928(19)	176(4)	*-x+2, -y+1, -z+1*

Table S5

Values of binding constants of silver(I) complexes **1 – 5** with DNA.

Complex	UV-Vis titration		Fluorescent titration				
	K_b (M^{-1})	ΔG^o (kcal/mol)	K_{sv} (M^{-1})	Hypochromism (%)	K_q (M^{-1}/s)	K_A (M^{-1})	n
1	$1.03 \cdot 10^4$	-5.5	$(2.62 \pm 0.10) \cdot 10^3$	19.7	$2.62 \cdot 10^{11}$	$4.23 \cdot 10^4$	1.30
2	$1.22 \cdot 10^3$	-4.2	$(1.72 \pm 0.05) \cdot 10^3$	13.0	$1.72 \cdot 10^{11}$	$9.56 \cdot 10^3$	1.18
3	$7.00 \cdot 10^3$	-5.2	$(2.65 \pm 0.05) \cdot 10^3$	20.8	$2.65 \cdot 10^{11}$	$2.78 \cdot 10^3$	1.01
4	$3.74 \cdot 10^3$	-4.9	$(2.06 \pm 0.10) \cdot 10^3$	13.7	$2.06 \cdot 10^{11}$	$1.12 \cdot 10^3$	0.92
5	$1.20 \cdot 10^4$	-5.5	$(3.23 \pm 0.06) \cdot 10^3$	24.6	$3.23 \cdot 10^{11}$	$1.47 \cdot 10^3$	0.91